Step by step development of HIRM-KW: a field-scale runoff model

Domenico Ditto[1], Mattia Sanna[1], Lodovico Alfieri[1], Mattia Fumagalli[1], Marco Acutis[1]*

[1] Department of Agricultural and Environmental Sciences (**DiSAA**) - University of Milan, Italy
[*] Corresponding author: domenico.ditto@unimi.it

Abstract: *One of the major causes of land degradation and loss of fertility is the soil erosion due to water runoff. In Italy, the 77% of the territory is estimated to be threatened by accelerated erosion, because of both its natural structure and anthropic action. This leads to the need of developing modelling tools able to provide useful information for runoff risk assessment. This paper presents a detailed description of HIRM-KW (Hydrological Infiltration Runoff Model), a physics-based hydrological model for simulating the dynamics of water runoff and infiltration in lowland soils. The model was developed by coupling a Kinematic Wave model with the Smith-Parlange infiltration theory and by making use of the basic laws of motion. Moreover, it was built up step by step in order to obtain a system of equations, lending itself to numerical treatment. HIRM-KW performances were evaluated, for demonstration purposes, by comparing the results of three simulations with corresponding outputs provided by the EUROSEM (European Soil Erosion Model), resulting in a good degree of agreement. HIRM-KW is implemented by a freeware software and the executable program can be requested to the Authors.*

Keywords: *Kinematic-Wave equations, infiltration-runoff processes, physics-based models, soil erosion, numerical methods.*

1. INTRODUCTION

Soil erosion by water is one of the major issues of land conservation and it can be effectively limited by adopting efficient agricultural techniques (EC 232, 2006), as a consequence the knowledge of soil hydrological response to water dynamics is essential. Such knowledge is provided, for example, by inflow/outflow models, which can be applied to lowland soils, often being affected by problems connected to excess-water management, small-scale border or rainfall irrigation. Moreover, these models can be exploited to deal with water storage decreasing and erosion caused by the reduction of the cultivated soil layer and frequently occurring on steep slope lands.

The dynamic modelling of erosion is nowadays one of the most popular instrument to risk evaluation and identification, as it has been demonstrated that several problems concerning water runoff can be adequately treated by means of a variety of simplified physics-based models, such as the Diffusion-Wave model and the Kinematic-Wave model (Eagleson, 1970; Linsley *et al.*, 1982; Miller, 1984; Stephenson and Meadows, 1986; Chow *et al.*, 1988; Singh, 1996).

Actually, despite the simplifying assumptions required by the equations governing the numerous processes involved, fully physics-based models allow to improve the understanding of the system, being particularly efficient when applied at farmland scale or to small catchments. The most common approach for simulating the surface water movement is based on the Kinematic-Wave equation, often integrated with infiltration models. However, there are some restrictions to its applicability to lowland soils, due to the bed slopes problem. It is well known that the Kinematic-Wave model is unable to correctly reproduce water runoff dynamics, when the bed slope is very small or locally adverse. In order to overcome this problem, several approximate models based on Diffusion-Wave equation have been proposed (e.g. Singh, 1996).

The main objective of this paper is the step by step development of a software tool for field-scale runoff modelling. As the theoretical background of soil water dynamics involves advanced mathematical and physical concepts, which usually are not easy to be understood, are also provided (i) a review of the basic physics of water surface runoff and other related processes and (ii) numerical methods for their practical application in hydrological modelling.

In particular, we provide an exhaustive of HIRM-KW (*Hydrological Infiltration Runoff Model*), a physics-based hydrological model, for simulating the dynamics of surface runoff and water infiltration at field scale, over a single plane or over a cascade planes. The model was built up step by step in order to obtain an system of equations, lending itself to numerical treatment, and the main mathematical details are explicitly reported in the main text and in the appendices, since they are not usually outlined in the documentation of the most popular runoff models.

The theoretical model elaboration has gone hand in hand with the development of a freeware software, whose main features are simplicity and flexibility, granted by an object-oriented software architecture. The numerical libraries of the program are entirely written in C++ (see e.g. Press *et al.*, 2002; Lippman et al., 2000, Malik, 2011) and they can be easily interfaced with a C# graphical front-end for the management of input/output data (see e.g., Nash, 2010). This led to the creation of an up-to-date software framework, allowing the assembling of more complex hydrological models and the integration of its main computational components into other simulation programs like the ARMOSA simulation crop model (Perego et al., 2013).

Section 2 describes the basic physical notions of soil water dynamics, implemented by HIRM-KW. Section 3 describes the HIRM-KW step by step development, clarifying how the equations of motion are first derived and assembled into a physical-mathematical model, and then numerically solved by non-linear finite difference methods.

Section 4 shows, for demonstration purposes, the results of some infiltration and runoff simulations, which in the end were compared to the corresponding EUROSEM outputs (Morgan *et al.*, 1998).

2. BASIC PHYSICAL THEORIS

2.1 Kinematic Wave flow routing models

The equations of motion for the surface runoff are usually derived by the well-known *De Saint-Venant* dynamic equations. They represent the mathematical expressions of the conservation laws for mass and momentum and they form a system of two Partial Differential Equations (PDE) of first order of the hyperbolic type. Such equations are highly nonlinear and analytical solutions can be obtained only in very few cases (see e.g. Yen and Chow *et al.*, 1974; Miller, 1984; Chow *et al.*, 1988; Brass, 1990; Singh, 1996). Starting from these equations, the most general models for simulating the surface runoff motion, are those based on the Dynamic Wave equations (for mathematical details, see Eqs. from (A.1.1) to (A.1.9)). Due to their hight non-linearity, a first approximation is usually adopted, represented by the Diffusion Wave models, from wich in turn an approximate form can be derived.

In Appendix A.2 the derivation of the Diffusion Wave equation from the Dynamic Wave model is reported (see Eqs.(A.2.1)-(A.2.4)), while in Appendix A.3 mathematical details are listed, to obtain its approximate form (see Eqs. from (A.3.1) to (A.3.8)).

Despite such approximations, still the Diffusion Wave model is highly non-linear, being not easy to be used for dynamic modelling of overland flow. Consequently, a further approximation is usually adopted, being referred to as Kinematic Wave models (for mathematical details, see Eqs. from (A.4.1) to (A.4.6)).

HIRM-KW was developed by coupling a Kinematic-Wave model with the Smith-Parlange infiltration theory and by making use of the basic laws of motion.

The main features of the Kinematic Wave model, implemented by HIRM-KW, are reported in the fellowing subsections.

2.1.1. *Kinematic-Wave model for overland flow*

As discussed in Appendix A, the Kinematic-Wave equation (Eq.(A.4.6)) is based on a combination of the full continuity equation with the momentum equation for steady, uniform flow.

Considering a channel with large rectangular section A, width W and height $h(x,t)$ equal to the depth of flow, such as $W \gg h$, this channel can be assimilated to an inclined plane, where the wetted perimeter P and the hydraulic radius R_a can be approximated by $P = 2h + W \approx W$ and $R_a = A/P \approx h$. In other words, the wetted perimeter is approximately equal to the plane width and the hydraulic radius is reduced to the flow depth h (see e.g. Miller, 1984; Chow *et al.*, 1988; Singh, 1996).

If the Kinematic-Wave approximation is applied, the friction slope S_f and the bed S_0 slope are approximately equal, while the average speed $U(x,t)$, of the flow in the direction of motion simplifies to

$$U \approx \frac{N\sqrt{S_0}}{P^{\beta-1}} A^{\beta-1} \equiv \alpha_0 h^{\beta-1} \tag{1}$$

where α_0 is a roughness coefficient.

If the *Chezy* relationship is used, then $\alpha_0 \equiv C\sqrt{S_0}$ has the dimensions of $[L^{1/2}/T]$; on the other hand, if the *Manning* relationship is used, then $\alpha_0 \equiv \sqrt{S_0}/n$ has the dimensions of $[L^{1/3}/T]$.

Eq.(A.4.6), can then be written as

$$\frac{\partial h}{\partial t} + \beta\alpha_0 h^{\beta-1}\frac{\partial h}{\partial x} = \tilde{q}_E \tag{2}$$

and Eq.(A.4.2) simplifies to

$$Q = UA \simeq \alpha_0 W h^{\beta} \tag{3}$$

where $Q(x,t)$ has the dimensions of a volumetric flow rate $[L^3/T]$.

Eq.(2) is referred to as the *Kinematic-Wave approximation* and it is used in hydrological models for simulating overland flow *runoff*.

2.1.2. *Wave celerity of the Kinematic-Wave model*

The wave celerity c_K $[L/T]$ of the Kinematic-Wave model (Eq.(2)) can be obtained from Eq.(A.4.8), based on the velocity law adopted; thus, resulting

$$c_K(h) \equiv \beta U \equiv \beta\alpha_0 h^{\beta-1} \tag{4}$$

2.1.3. *Criterion of applicability of the Kinematic-Wave model*

Analysing runoff characteristics in different flow conditions, Woolhiser et al. (1967, 1970), Singh, (1996,

2002) and Moramarco et al (2002), concluded that the Kinematc-Wave assumption is accurate within an error of 10%, if the kinematic flow number K is greater than 20 and the Froude number F_r is greater than $1/2$, leading to the application criterium ${F_r}^2 K > 5$.
Several authors confirmed Woolisher's conclusions, showing that Eq.(2) provides a good approximation for describing surface runoff and erosion in most flow conditions (Chow *et al.*, 1988; Brass, 1990; Singh, 1996). Furthermore, it has been demonstrated that when $S_0 < 0.02$ or $S_0 > 0.10$, the kinematic assumption is violated (Henderson, 1966; Govindaraju *et al.*, 1988a,b). Even if this approach introduces a strong simplification, it has been successfully applied in several practical cases (see e.g., Ogden and Julien, 1993), including the numerical analysis of the water flux of macropores in soil proposed by Alaoui et al, (2003).

2.2 Rainfall intensity excess (or Total Runoff)

In Eq.(2), the lateral flow, $\tilde{q}_E(x,t)$ $[L/T]$ is a surface flow per unit width. When it refers to a plane, it may include different terms, such as net rainfall, R_{NET}, irrigation, melting snow, etc. Assuming bare soil, absence of irrigation inputs and neglecting water evaporation from the soil surface, the term $\tilde{q}_E(x,t)$ represents the difference between *rainfall intensity* $i(x,t)$ and *infiltration rate* $f(x,t)$:

$$\tilde{q}_E(x,t) = \frac{q_E(x,t)}{W} \equiv \frac{i(x,t)-f(x,t)}{W}, (W \equiv 1\ [L]) \qquad (5)$$

Eq.(5) holds in general; however, considering relatively small surfaces (e.g. agricultural fields) with homogeneous soils, the x-dependence of both i and f is negligible. As a consequence, it can be approximated as $\tilde{q}_E(x,t) \approx [i(t) - f(t)]/W$, where $i(t) = dR_{NET}/dt$ and $f(t) = dF/dt$. The term $F(t)$ $[L]$ defines the cumulative infiltration, while $\tilde{q}_E(x,t)$ is generally known as *rainfall intensity excess* per unit width or *total runoff*.
It is important to underline that this approximation is not valid in the case of a river basin.

2.3 Distribution of rainfall periods

The set of rainfall periods required by runoff simulation is displayed in Fig.1, where the rainfall intensity of the j^{th} period is given by $i_j = P_j/D_j$ $[L/T]$, P_j representing the precipitation amount and D_j the corresponding time interval.
Accordingly, the *maximum rate of rainfall inflow* is defined as the maximum specific intensity $i_{max} = P_{max}/D_{jmax}$, where P_{max} is the maximum precipitation amount occurring.
Rainfall events are subsequently transformed into a distribution of periods with a constant timestep (Δt) of the order of a few minutes, while the rainfall intensity $i(t)$ is calculated as $R_{NET}/\Delta t$, where R_{NET} $[L]$ is the net rainfall reaching the soil surface.

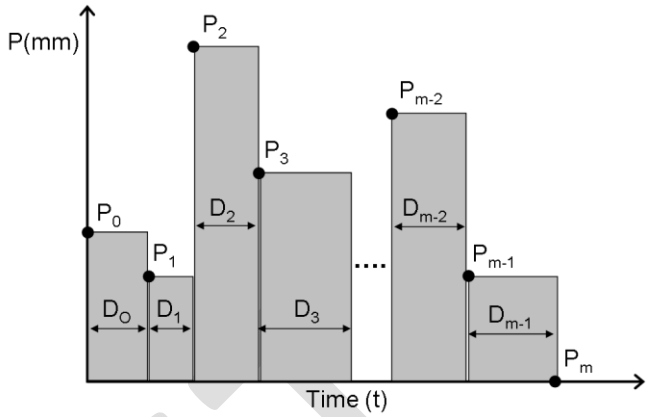

Fig.1 - Example of rainfall hyetograph used in the HIRM-KW model. The ordinate shows the amount of rain P_j refers to the *j-th* event duration D_j.

The net rainfall is usually estimated by a hydrological balance equation, involving several agro-meteorological processes:

$$R_{NET} \cong P - \left(E_P + T_p + Int + \cdots\right) \qquad (6)$$

where P $[L]$ is the natural rainfall; $E_p + T_p$ is the water lost by evapotranspiration ET_P; Int $[L]$ is the amount of water intercepted by standing vegetation.
Many models are available to compute interception as a static or dynamic process but they are not considered here. Moreover, the amount of water lost by ET_P during a rain event turns out to be negligible, therefore it is not taken into account.

2.4 Soil water infiltration models

In this subsections, the fundamentals of infiltration theory are employed to derive an analytical function for both the potential *infiltration rate* $f(t)$ end the *cumulative infiltration depth* $F(t)$, and to obtain the effective capillary drive term $G(\theta_I, \theta_0)$, through the Brooks and Corey equation.

Smith-Parlange cumulative infiltration model

The function $F(t)$ $[L]$ is the *cumulative infiltration* depth and it is defined as:

$$F(t) = \int_0^t f(t)dt \qquad (7)$$

where $f(t)$ $[L/T]$ is the *infiltration rate*.
Several physics-based models relate $F(t)$ to *sorptivity* S_P $\left[L/T^{1/2}\right]$ and *hydraulic conductivity at saturation* K_s $[L/T]$, allowing to estimate these two quantities from infiltration data and by applying Eq.(7). One of the possible formulations of this relationship is given by the implicit equation proposed by *Smith* (2002):

$$F(t) \cong K_s t - \frac{{S_P}^2}{2K_s}\left(e^{-\frac{2K_s F(t)}{{S_P}^2}} - 1\right) \qquad (8)$$

Being Eq.(8) an implicit equation, $F(t)$ can be obtained by applying iterative methods (we adopt the Newton-Raphson method).

Smith-Parlange infiltrability model

One of the most common approaches for estimating *infiltrability* $f_c(t)$ $[L/T]$ (also known as *infiltration capacity*), is through the application of the *Smith-Parlange* model (Parlange 1971, 1972, 1975a, b; Smith and Parlange, 1978; Parlange *et. al.*, 1982; Smith, 2002) with three parameters:

$$f_c(t) \cong K_s\left(1+\frac{\gamma}{e^{2\gamma K_s F(t)/S_P{}^2}-1}\right), \quad \gamma>0 \tag{9}$$

Clearly, $f_c(t)$ is obtained by substituting $F(t)$, calculated via Eq.(8).

It is worth to underline that, the best fit value for γ ranges from 0.80 to 0.85 (Parlange et al., 1982; Smith et al., 2002). Moreover, the *sorptivity* S_P in Eqs.(8)-(9) is defined as:

$$S_p=\sqrt{2K_sG(\theta_I,\theta_0)\Delta\theta}\equiv\sqrt{2K_sB} \tag{10}$$

where

$$\begin{aligned} &B=G(\theta_I,\theta_0)\Delta\theta.\\ &\Delta\theta\equiv(\theta_S-\theta_I)\equiv\Phi(S_S-S_I)\,,\\ &S_S=\theta_S/\Phi\,,\quad S_I=\theta_I/\Phi\,, \end{aligned} \tag{11}$$

Φ $[L^3/L^3]$ is the effective soil *porosity*; θ_0 $[L^3/L^3]$ is the water content at the soil surface; θ_S $[L^3/L^3]$ and θ_I $[L^3/L^3]$ are the saturated and initial soil water content, respectively; S_S and S_I are the relative and initial soil saturation, respectively; $\Delta\theta$ is the initial soil water content deficit; B [L], is the deficit of saturation of the soil. The hydraulic parameters K_s, G, θ_S, θ_I and Φ, are related to *sorptivity* through Eq.(10).

The term G $[L]$ is the integral of the *effective capillary drive* through the saturated front under initially dry conditions and it was defined (Ogden et al., 1997) as:

$$G(\theta_I,\theta_0)=\int_{\psi_I}^{0}K_r(\psi)d\psi\,,\quad K(\psi)=K_sK_r(\psi) \tag{12}$$

where $K(\psi)$ $[L/T]$ and $K_r(\psi)$ $[L/T]$ are the *hydraulic conductivity* and the *relative unsaturated hydraulic conductivity* functions; ψ $[L]$ is the *soil water capillary pressure head* (i.e. the negative of *matric suction head*) and ψ_I $[L]$ is the *capillary pressure head* at at $\theta=\theta_I$.

Evaluation of effective capillary drive term

Several analytical expressions of G exist, depending on the form of soil water retention and unsaturated conductivity functions (Morel-Seytoux et al., 1996 and 1999; Ogden et al., 1997; Smith et al., 2002). G also depends on the *initial capillary suction* ψ_I $[L]$ and it can be estimated knowing $K(\psi)$.

For example, using *Brooks* and *Corey* equations (Brooks and Corey, 1964)

$$\begin{cases} K(\psi)=K_s(\psi_B/\psi)^{3+2/\lambda}; & if\ \psi\le\psi_B\\ K(\psi)=K_s; & if\ \psi>\psi_B\\ \vartheta=\frac{\theta-\theta_r}{\theta_s-\theta_r}=\left(\frac{\psi_B}{\psi}\right)^{\lambda}\,; & if\ \psi\le\psi_B\\ \vartheta=1; & if\ \psi>\psi_B \end{cases} \tag{13}$$

and substituting in the Eq.(12), Ogden et al (1997) has proposed the following expression of G (see Appendix A.5 for details):

$$G(\theta_I,\theta_0)=-\frac{\psi_B}{\lambda}\left(\frac{1-\vartheta_I{}^{3+1/\lambda}}{3+1/\lambda}\right) \tag{14}$$

where $\vartheta_I=(\theta_I-\theta_r)/(\theta_s-\theta_r)$ is the *relative initial volumetric water content* (dimensionless); ψ_B $[L]$ is the bubbling pressure head; θ_r $[L^3/L^3]$ is the residual water content of the soil profile, and λ (dimensionless) is the pore-size distribution index.

In this study we assuming that the initial water content is equal to the residual saturation (i.e. $\psi_I=\infty, \vartheta_I=0$), then the *effective net capillary drive* G_0 $[L]$, can be approximated by the following formula (Ogden et al., 1997; Morel-Seytoux et al 1996 and 1999; Rawls *et al.*, 1982; Smith et al., 2002):

$$G_0\cong-\psi_B\frac{(2+3\lambda)}{(1+3\lambda)} \tag{15}$$

holding after a long rain break. ψ_B and λ can be also obtained by fitting the *Brooks* and *Corey* equation to an experimental data set (Rawls et al., 1982). In Eqs.(12)-(15) the sign of the terms ψ , ψ_I and ψ_B has to be considered as negative.

In HIRM-KW the quantity G_0 may be either assigned as an input parameter or evaluated by means of Eq.(15). $G(\theta_I,\theta_0)$ could also be calculated by using other conductivity functions (e.g. Mualem, 1976; Van Genuchten, 1980; Rawls and Pachepsky, 2004).

The soil-water characteristic (ψ_I , ψ_B and K_s) can be indirectly estimated from the physical properties of the soil (i.e., clay, sand, silt, organic matter soil density), applying pedotransfer functions (e.g. Saxton *et al.*, 1986; Acutis *et al.*, 2003; Rawls and Pachepsky, 2004).

Moreover effective porosity, appearing in Eqs.(11), can be estimated from real and apparent soil density.

Infiltration capacity during a rainfall pause

Eqs.(7)-(11) hold in general, when $i(t)\ge K_s$; however, during a real precipitation event different periods may exist, with $0\le i(t)<K_s$ (i.e., almost absence of rain).

As long as the water remains on the surface (satisfying the conditions of existence of the infiltration capacity $f_c(t)$), the Smith-Parlange theory still covers small or absent rainfall events of very short duration.

On the contrary, when longer dry periods occur, part or the whole soil surface is free from water, the process of water redistribution in soil occurs and the theory is no longer valid.

3. HIRM-KW FIELD-SCALE RUNOFF MODEL

3.1 Unified equations of the model

As already stated, in HIRM-KW, the Kinematic Wave model is coupled with the two-parameters Smith-Parlange infiltration model (9). Consequently, considering a single runoff plane (see Fig.2), the physical model described in the previous sections can be summarized by the following set of equations:

$$\begin{cases} S_P \cong \sqrt{2K_s G_0(\theta_S - \theta_I)} \\ F(t) \cong K_s t - \frac{S_P{}^2}{2K_s}\left\{e^{\left(-\frac{2K_s F(t)}{S_P{}^2}\right)} - 1\right\} \\ f(t) = K_s \frac{e^{\left(\frac{2K_s F(t)}{S_P{}^2}\right)}}{e^{\left(\frac{2K_s F(t)}{S_P{}^2}\right)} - 1} \\ \tilde{q}_E(t) = \frac{[i(t) - f(t)]}{W}, (W \equiv 1\,[L]) \\ \frac{\partial h}{\partial t} + \beta\alpha_0 h^{\beta-1}\frac{\partial h}{\partial x} = \tilde{q}_E \\ Q(h) = W\alpha_0 h^{\beta} \end{cases} \quad (16)$$

where β ($\equiv 5/3$), α_0, is the Manning roughness coefficient and a Smith-Parlange model with two parameters is adopted, setting $\gamma \equiv 1$ in Eq.(9).

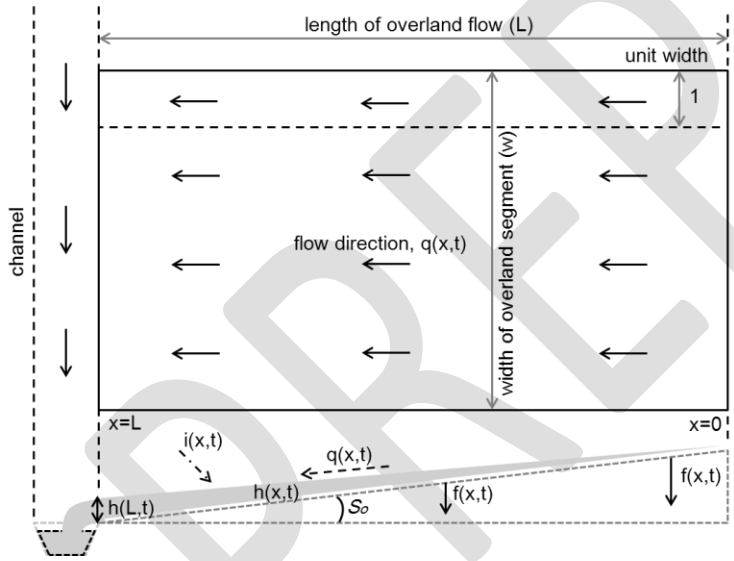

Fig.2 – Dynamics of surface runoff in a plane of the length L and width W creating an excess of rainfall (q), conveyed in an open channel.

The evaluation of the overland flow is then obtained starting from the set of equations (16) and looking for solutions of the type $h(x,t)$ in the domain of variation $\Omega = \{0 \le x \le L;\ 0 \le t \le T_{MAX}\}$. Values of $h(x = L, t)$ are finally employed to calculate the outflow rate $Q(x = L, t)$ through Eq.(3). Eq.(3) applies even if the plane is the first of a sequence of planes and the conditions specified by the set equations (16) can be extended to a sequence of cascade planes (see Fig.3).

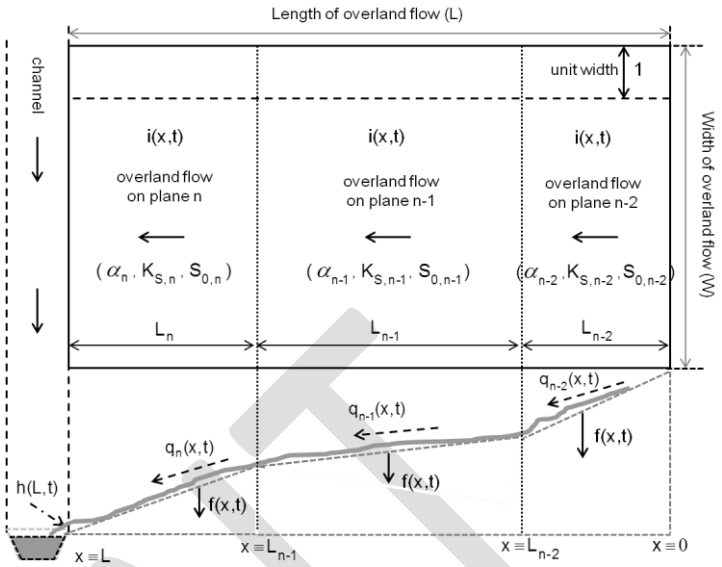

Fig.3 – Dynamic of surface runoff for a set of planes of equal width (W) connected in cascade where the runoff is conveyed in an open channel.

3.1.1. *Equations in dimensionless form*

The set of equations (16) are expressed in dimensional form. However, many internal calculations of our model, can be carried out by using variables in dimensionless form (with appropriate scaling factors). For clarity sake, we recall that the formulation of a problem in dimensionless form requires to switch a reference system of units intrinsic to the same problem (Bridgman, 1923); apart from that, any formal difficulty arising from the change of variables is overcome by some major advantages:

1. simpler mathematical relationships, because of the reduction of the number of parameters;
2. calculation efficiency;
3. assessment of the relative weights of the terms in the equations and of their influence on the process;
4. possibility of establishing comparison criteria: the values of the dimensionless variables are independent of the measurement system;
5. the possible appearance of a small parameter value would indicate the minor role of the terms containing it.

We define the new dimensionless variables (denoted by the symbol ~) by assuming:

$$\tilde{t} = \frac{K_s t}{B},\ \tilde{x} = \frac{K_s x}{\alpha_0 \beta B},\ \tilde{f} = \frac{f}{K_s},$$
$$\tilde{F} = \frac{F}{B},\ \tilde{\imath} = \frac{i}{K_s},\ \tilde{h} = \frac{h}{B} \quad (17)$$
$$\tilde{Q} = \frac{Q}{\alpha_0 W B^{\beta}},$$

where α_0 is the roughness coefficient and $B \cong G_0(\theta_s - \theta_I)$ $[L]$, the deficit of saturation of the soil are given by Eqs.(11).

The set of equations (16) become, in the case of

dimensionless variables:

$$\begin{cases} \tilde{F} = \tilde{t} - \{e^{-\tilde{F}} - 1\} \\ \tilde{f} = \frac{e^{\tilde{F}}}{e^{\tilde{F}}-1} \\ \frac{\partial \tilde{h}}{\partial \tilde{t}} + \tilde{h}^{\beta-1}\frac{\partial \tilde{h}}{\partial \tilde{x}} = (\tilde{\imath} - \tilde{f}) \\ \tilde{Q}(\tilde{x},\tilde{t}) = \tilde{h}(\tilde{x},\tilde{t})^{\beta} \end{cases} \quad (18)$$

In HIRM-KW the surface runoff is modelled by numerically solving the system of equations (18), according to the *Manning* law of resistance and the criterion of applicability of the Kinematic-Wave model (see Appendix A.4.4).
It is worth to observe that, in dimensionless form, the number of equations is reduced to four.

3.1.2. *Initial and boundary conditions*

Before the beginning of the rain event, HIRM-KW sets an initial soil water content θ_I; moreover, for a single plane of length L the initial (IC) and boundary (BC) conditions are identical (see Fig.2). Therefore

$$\begin{cases} IC: h(x,0) = 0;\ q_E(x,0) = 0; \quad 0 \le x \le L \\ BC: h(0,t) = 0;\ q_E(0,t) = 0;\ \ 0 \le t \le T_{MAX} \end{cases} \quad (19)$$

where T_{MAX} is the total duration of the rainfall event. Q $[L^3/T]$ can be calculated by applying Eq.(3) at $x = L$, then obtaining:

$$Q(L,t) \equiv W\tilde{Q}(L,t) \equiv \alpha W[h(L,t)]^{\beta} \quad (20)$$

where W is the width of the plane; $\tilde{Q}$ is the flow rate per unit width and $\alpha \equiv \frac{1}{n}\sqrt{S_0}$.
In the case of a sequence of planes (Fig.2), the boundary conditions at each must be defined. Actually, being $\tilde{Q}_{u,n}$ the unitary flow of plane n at the upper contour (u) and $\tilde{Q}_{l,n-1}$ the unitary flow of plane $n-1$ at the lower contour (l), it is possible to apply Eq.(20) at the intersection point $x_u \equiv x_l \equiv L_{n-1}$ (being $W_{u,n}$ and $W_{l,n-1}$, the plane widths), obtaining:

$$\tilde{Q}_{u,n}(x_u,t)W_{u,n} \equiv \tilde{Q}_{l,n-1}(x_l,t)W_{l,n-1}, \quad t > 0,\ 0 \le x_u \le L_n,\ 0 \le x_l \le L_{n-1} \quad (21)$$

and consequently, following Woolhiser *et al.* (1970):

$$\tilde{Q}_{u,n}(x_u,t) = \tilde{Q}_{l,n-1}(x_l,t)\frac{W_{l,n-1}}{W_{u,n}} \quad (22)$$

Focusing on the flow depth h at the intersection point, the inflow heights of flow $h_{u,n}(x_u,t)$ at the lower plane L_n, and the outflow heights of flow $h_{l,n-1}(x_l,t)$ at the upper plane L_{n-1}, coincide, except for a multiplication factor. By adapting Eq.(20) into Eq.(22), we have:

$$h_{u,n}(x_u,t) = \left(\frac{\alpha_{u,n-1}W_{l,n-1}}{\alpha_{l,n}W_{u,n}}\right)^{\frac{1}{\beta}} h_{l,n-1}(x_l,t) \quad (23)$$

Eq.(23) implies that the same law of *Manning's* resistance holds at the two planes.
In the particular case of two consecutive planes, with the same width W, Eqs.(21) becomes $\tilde{Q}_{u,n}(x_u,t) = \tilde{Q}_{l,n-1}(x_l,t)$ and, as a consequence, Eq.(23) can be written as follows:

$$h_{u,n}(x_u,t) = \left(\frac{\alpha_{u,n-1}}{\alpha_{l,n}}\right)^{\frac{1}{\beta}} h_{l,n-1}(x_l,t) \quad (24)$$

where $\alpha_{l,n}$ and $\alpha_{u,n-1}$ are the roughness coefficients for the lower (n) and the upper ($n-1$) plane, respectively.

3.1.3. *Global Volume Balance (GVB)*

When a modelling process exploits any numerical solution of differential equations, the volume balance between system *Inflow* and *Outflow* system must be evaluated. In our case, such balance can be written as:

$$\frac{dV}{dt} = Aq_E(t) - Q_s(x,t) \equiv Ai(t) - [Af(t) + W\tilde{Q}_s(x,t)] \quad (25)$$

where $q_E(t) = i(t) - f(t)$ is the intensity of rainfall excess $[L/T]$, $A = LW$, L and W are respectively: surface $[L^2]$, length $[L]$ and width $[L]$ of an overland flow on a rectangular surface.
Moreover, $\tilde{Q}_S$ $[L^2/T]$ is the flow intensity per unit width W, which can be calculated by means of the followining equation (Huber and Dickinson, 1988):

$$Q_s(x,t) \equiv W\tilde{Q}_s(x,t) = W\alpha_0[h(x,t) - h_d]^{\beta} \quad (26)$$

where α_0 is the roughness coefficient; h_d $[L]$, is called *depression storage depth* and it takes into account the fraction of water remaining on the ground surface, when no infiltration occurs.
In HIRM-KW h_d can be calculate as $h_d = e^{(-6.66+0.27RFR)}$ (Auerswald, 1992), where RFR [L/L], is a downslope roughness ratio based on field measurement and published table of experimentally determined values (Morgan et al., 1998; Folly et al., 1999).
Water in depression storage does not directly contribute to overland flow runoff because it either evaporates or infiltrates later.
Eq.(25) can be integrated between the starting time (t_{INI}) and the final time (t_{END}) of the rainfall event, thus obtaining the balance equation in integral form:

$$\Delta V \equiv A\int_{t_{INI}}^{t_{END}} i(L,t)dt - \int_{t_{INI}}^{t_{END}} [Af(L,t) + W\tilde{Q}_s(L,t)]dt \quad (27)$$

Although Eq.(27) is expressed in $[L^3]$, it is often practical to express it in terms of flow depth Δh $[L]$. Moreover, being

$$\frac{dV}{dt} \equiv A\frac{dh}{dt},\ \ \tilde{Q}_s(x,t) \equiv \frac{Q_s(x,t)}{W} \quad (28)$$

Eq.(27) can be written as

$$\Delta h \equiv \int_{t_{INI}}^{t_{END}} i(L,t)dt - \int_{t_{INI}}^{t_{END}} \left\{f(L,t) + \frac{W\alpha_0}{A}[h(L,t) - h_d]\right\}^{\beta} dt \quad (29)$$

where $i(L,t)$, $f(L,t)$ and $\tilde{Q}_s(L,t)$ are the rainfall intensity [L/T], the infiltration rate [L/T] and the flow intensity per unit length [L²/T], respectively. They are all evaluated at $x = L$, for the entire rainfall duration.
Finally, in the calculation of the percentage of *Global Volume Error* (% GVE), we used the formula

$$GVE = 100\left|\frac{R_{NET}-\Delta h}{R_{NET}}\right| \quad (30)$$

where R_{NET} $[L]$ is the net rainfall reaching the soil surface.
Eqs.(27), (29) and (30) are exploited to control the Global Volume Balance (GVB) of HIRM-KW simulations (see Section 4).

3.2 Assumptions and limitations

If the applicability conditions of the Kinematic-Wave model defined in the Section 2.1.3 are satisfied, then the theory described in Section 2.1 can be a valid simplification for surface runoff.
The validity of the hydrological model (16) however, is subject to some limitations:

1. precipitation occurs without interruption and it is constant over the entire space integration domain x, consequently rainfall intensity changes in time but not in space (i.e. $i(x,t) \approx i(t)$);
2. the theory described in the Section 2.4 can be applied when the rainfall intensity is greater than the hydraulic conductivity at saturation (i.e. $i(t) > K_s$, according to the Hortonian overland flow approach);
3. the model does not take into account the water redistribution process; therefore, the effective capillary drive (G), can be assigned parameter or can be estimated by Eq.(15);
4. the friction slope S_f coincides with the topographic slope S_0 (see Eq.(A.4.1));
5. the hydraulic conductivity (K), effective capillary drive (G) and the infiltration rate (f) are constant over the space integration domain on the plane; furthermore K and G does not vary with the depth z, and we assume only one layer of homogeneous soil, for which $K(x,z) \approx K_s$ and $f(x,t) \approx f(t)$;
6. Manning roughness parameter n is constant over the entire space integration domain x and it is estimated by using Eq.(A.4.13);
7. during the whole rainfall absence of interception is assumed (i.e. $Int \approx 0$), Eq.(6) then reduces to $R_{NET} \approx P$;
8. an initial soil water content (θ_I) is assumed constant over the depth of wetting but varies between stoms, being the runoff surface regular in shape with width W, length L and bed slope S_0.
9. the model (16) does not consider erosion, rill, presence of surface snow and percolation losses.

3.3 Numerical solutions of the model

The equation to be solved (Eq.(2)) is a first order hyperbolic PDE, nonlinear in h, simulating the change of water depth (h) on the grid plane (x,t). Analytical solutions exist in very few special cases and most of them are of little practical interest. As a consequence, the solution is usually numerically sought, by applying the Finite Differences (FD) method or the Finite Elements (FE) method.
In HIRM-KW the runoff simulation is performed by seeking a solution $h(x,t)$ for the flow rate $Q(x,t)$ (Eq.(3)) and then solving Eq.(2) with FD methods (see Appendix B). HIRM-KW allows to use both a 3-points *linear* schemes (Fig.B.1) and a 4-points *nonlinear* schemes (Fig.B.2). Figs.(B.1) and (B.2) represent the uniform mesh solution of the *Finite Difference Backward* scheme (FDB) used to calculate the partial derivatives of Eqs.(2) (Singh, 1996; Chow *et al.*, 1988; Holden and Stephenson, 1988, 1995; Wood, 1993).
Applying the *FD* methods, Eq.(2) in the *dimensionless form* (see Eqs.(17)) can be re-written as follows (omitting the symbol ~ here and after in the text):

$$\frac{\partial h}{\partial t} + h^{\beta-1}\frac{\partial h}{\partial x} = q_E \quad (31)$$

or in the equivalent form

$$\frac{\partial h}{\partial t} + \frac{1}{\beta}\frac{\partial h^{\beta}}{\partial x} = q_E \quad (32)$$

where $q_E \equiv (i-f)$.

Linear 3-points FDB scheme for Kinematic-Wave Eq.(31):

By replacing Eq.(B.1.1) into Eq.(31), we have a system of linear equations in the unknown h_{i+1}^{j+1}, whose explicit solution is given by the formula (Chow *et al.*,1988; Kazezyılmaz-Alhana *et al.*, 2005):

$$h_{i+1}^{j+1} = \frac{h_{i+1}^{j} + C_r\, h_i^{j+1} + \bar{q}_E \Delta t}{1+C_r},\ C_r \equiv c_k\frac{\Delta t}{\Delta x} \equiv \bar{h}_C{}^{\beta-1}\frac{\Delta t}{\Delta x} \quad (33)$$

where $C_r < 1$ is the *Courant numbe*r; c_k is the *wave celerity* and $\bar{h}_C \approx 0.5\left(h_i^{j+1} + h_{i+1}^{j}\right)$.

Linear 3-points FDB scheme for Kinematic-Wave Eq.(32)

Replacing Eq.(B.2.1) into Eq.(32), we have a system of linear equations in the unknown h_{i+1}^{j+1} whose explicit solution is given by:

$$h_{i+1}^{j+1} = h_{i+1}^{j} - Ah_{i+1}^{j} + Bh_i^{j} + \bar{q}_E\,\Delta t \quad (34)$$

where

$$A \equiv \frac{\Delta t}{\beta \Delta x}\left(h_{i+1}^{j}\right)^{\beta-1},\ B \equiv \frac{\Delta t}{\beta \Delta x}\left(h_i^{j}\right)^{\beta-1} \quad (35)$$

Numerical stability of schemes (33) and (34)

The numerical stability condition to be satisfied in the FDB schemes (33) and (34) is the Courant condition (Kibler and

Woolhiser, 1970):

$$\frac{\Delta t}{\Delta x} \geq c_{k,max} = \alpha_0 h_{max}^{\beta-1} \tag{36}$$

where $c_{k,max}$ is the maximum wave celerity for flow and h_{max} is the maximum flow depth. If L is the length of an overland flow (see Fig.2 and Fig.3), Δx can be approximated as $\Delta x \simeq \frac{L}{N}$, where $N \in \{10 \div 20\}$, such range being based on a numerical experimentation; however, this is an empirical criterion and it should be used just as basis guideline. Numerical scheme (33) is unconditionally stable but nonconvergent for any value of C_r (Singh, 1996).

Nonlinear 4-points FD scheme for Kinematic-Wave Eq.(31)

In HIRM-KW the solution of the Kinematic-Wave equation is obtained from a general implicit 4-points scheme, with weight factors for $h(x,t)$ and $Q(x,t)$, using Eq.(33) (or (34)) for the initial estimate of h. Substituting (B.3.1) and (B.3.2) into Eq.(31), we get the finite difference equation:

$$\begin{aligned} &a h_{i+1}^{j+1} + \lambda \left(h_{i+1}^{j+1}\right)^{\beta} = F \\ &F \equiv a h_{i+1}^{j} - (1-a)\left(h_i^{j+1} - h_i^{j}\right) + H + \Delta t q_E \end{aligned} \tag{37}$$

where

$$\begin{aligned} &\lambda \equiv b\,\frac{\Delta t}{\Delta x}\,, \\ &H = \lambda\left\{\left(h_i^{j+1}\right)^{\beta} - \frac{(1-b)}{b}\left[\left(h_{i+1}^{j}\right)^{\beta} - \left(h_i^{j}\right)^{\beta}\right]\right\} \end{aligned} \tag{38}$$

Eq.(37) is nonlinear in the unknown h_{i+1}^{j+1}, which can only be indirectly determined by solving, at each step, a system of linear equations (Press *et al.*, 2002; Epperson, 2002). Since F contains only known terms, the unknown h_{i+1}^{j+1} is calculated by the *Newton-Raphson method*, solving the equation $g\left(h_{i+1}^{j+1}\right) = 0$ and re-writing Eq.(37) as:

$$\begin{aligned} &v_{k+1} = v_k - \frac{g(v_k)}{g'(v_k)}, \\ &g(v_k) = \lambda {v_k}^{\beta} + a v_k - F, \\ &g'(v_k) = \frac{dg(v_k)}{dv_k} \end{aligned} \tag{39}$$

where $v_k = h_{i+1}^{j+1}$ is the value of h_{i+1}^{j+1} at the k^{th} iteration. The convergence of the iterative process of Eq.(39) is reached when $|v_{k+1} - v_k| \leq \varepsilon$, where ε is a dimensionless critical parameter.

A variant of FD scheme (37)

By replacing (B.3.3) and (B.3.4) into Eq.(31) (or Eq.(32)), we obtain the equation:

$$\begin{aligned} &\frac{1}{2} h_{i+1}^{j+1} + \lambda \left(h_{i+1}^{j+1}\right)^{\beta} = F \\ &F \equiv \frac{1}{2}\left(h_{i+1}^{j} + h_i^{j} - h_i^{j+1}\right) + H + q_E \Delta t \end{aligned} \tag{40}$$

where λ and H are defined by Eq.(38), $a \equiv 0.5$ and $0 \leq b \leq 1$. Since Eq.(40) is a particular case of Eq.(37) with $a = 0.5$, its solution is iteratively obtained, by adapting the method described by Eqs.(39). Eqs.(37) and (40) are *unconditionally stable*, with an accuracy of the second order for $b > 0.5$. It is worth to recall that accuracy is highly dependent on the choice of Δx and Δt in the implicit schemes (Ponce *et al.*, 1978; Smith, 1985; Thomas, 1995; Strikwerda, 2004). Eq.(40) may by also written in matrix form

$$\begin{aligned} &A_i h_i^{j+1} + B_i h_{i+1}^{j+1} = F \\ &F \equiv h_i^{j}\left(1 + \delta_{-} D_i^{j}\right) + h_{i+1}^{j}\left(1 - \delta_{-} D_{i+1}^{j}\right) + 2 q_E \Delta t \end{aligned} \tag{41}$$

where A_i, and B_i are given by

$$\begin{aligned} &A_i \equiv \left(1 - \delta_{+} D_i^{j+1}\right),\ B_i \equiv \left(1 + \delta_{+} D_{i+1}^{j+1}\right), \\ &\delta_{-} \equiv \frac{2(1-b)\Delta t}{\Delta x},\ \delta_{+} \equiv \frac{2 b \Delta t}{\Delta x}\,. \end{aligned} \tag{42}$$

and

$$\begin{aligned} &D_i^{j} \equiv \frac{1}{\beta}\left(h_i^{j}\right)^{\beta-1},\ D_i^{j+1} \equiv \frac{1}{\beta}\left(h_i^{j+1}\right)^{\beta-1}, \\ &D_{i+1}^{j} \equiv \frac{1}{\beta}\left(h_{i+1}^{j}\right)^{\beta-1},\ D_{i+1}^{j+1} \equiv \frac{1}{\beta}\left(h_{i+1}^{j+1}\right)^{\beta-1} \end{aligned} \tag{43}$$

For all the internal nodes, the system (41), can be consequently written as a tridiagonal square matrix which can be inverted by the *Thomas algorithm* (Thomas, 1995), allowing to solve the system:

$$\begin{bmatrix} 1 & 0 & 0 & \cdots & 0 & 0 \\ A_1 & B_1 & 0 & \cdots & 0 & 0 \\ 0 & A_2 & B_2 & \cdots & \cdots & 0 \\ \vdots & 0 & 0 & \cdots & \cdots & \vdots \\ 0 & \vdots & \vdots & \cdots & A_{N-1} & B_{N-1} \\ 0 & 0 & 0 & \cdots & 0 & 1 \end{bmatrix} \begin{bmatrix} h_0^{j+1} \\ h_1^{j+1} \\ h_2^{j+1} \\ \vdots \\ h_{N-1}^{j+1} \\ h_N^{j+1} \end{bmatrix} = \begin{bmatrix} F_0^{j} \\ F_1^{j} \\ F_2^{j} \\ \vdots \\ F_{N-1}^{j} \\ F_N^{j} \end{bmatrix} \tag{44}$$

3.4 The software tool HIRM-KW

The software tool HIRM-KW is based on the diagram presented in Fig.4, displaying the main processes involved during a dynamic simulation (see blocks A, B, C, D), including the surface runoff.

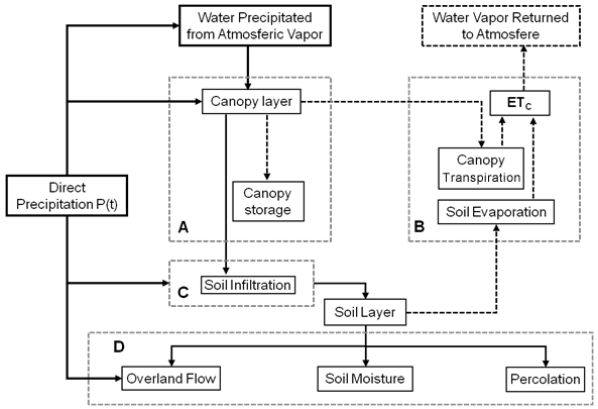

Fig.4 - Conceptual model of the main hydrological processes simulated by HIRM-KW.

It is important to underline that HIRM-KW takes into account only Hortonian overland flow (**D**) and soil infiltration (**C**). For what concerns its component-based architecture, the HIRM-KW logical structure is reported in Fig.5.

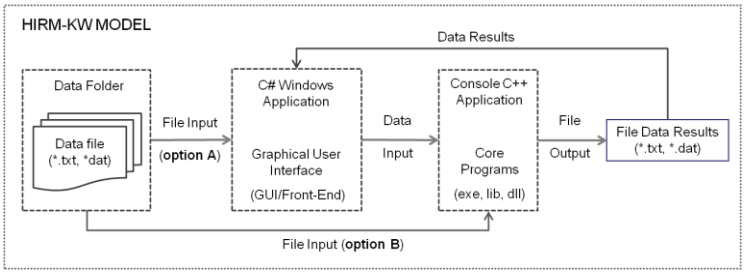

Fig.5 - Logical structure of the software tool HIRM-KW.

The software was deliberately developed to simulate few processes, being aimed at the dynamic simulation of infiltration-runoff in lowland soils characterized by very low slopes, and it is able to simulate surface runoff on a single field or on different fields, subject to rainfall events without interruption. In order to perform a simulation with HIRM-KW, first of all the following field-related parameters must be defined: width (W), length (L), topographic slope (S_0) and a *Manning's* surface roughness coefficient n_0. Moreover, physical and hydrological characteristics, namely the saturated hydraulic conductivity (K_s), and the effective net capillary drive (G_O) need to be known. The surface depression storage depth (h_d) instead is estimated using a surface soil roughness ratio (RFR). During a simulation, the runoff estimated by the Kinematic-Wave model starts when the infiltration capacity of the soil, evaluated with the *Smith-Parlange* equation, is exceeded. At the end of each simulation, the software provides several information: cumulative rainfall $R_C(t)$; flow depth $h(x,t)$; runoff expressed in terms of flow rate $Q(x,t)$; cumulative infiltration $F(t)$, infiltration rate $f(t)$, and infiltration capacity $f_c(t)$, obtained applying the two-parameters *Smith-Parlange* equation (Eq.(9), wiht $\gamma = 1$).

Tab.1 - Parameters calculated by the HIRM-KW model during a simulation.

GLOBAL VOLUME BALANCE		**RUNOFF SUMMARY**	
RAIN (mm)	Total Rainfall depth	**PRR** (mm/h)	Peak of Rainfall Rate
PSTO (mm)	Water moisture remaining on the plane	**TRUN** (min)	Time of Runoff
TINF (mm)	Total volume infiltration	**DRUN** (min)	Duration of Runoff
TRUN (mm)	Total volume Runoff	**TPFR** (min)	Time to Peak Flow Rate
TBAL (mm)	Total storage, infiltration/Runoff terms	**PFR** (mm/h)	Peak of Flow Rate
GVE (%)	% Global Volume Error		

The Global Volume Balance (GVB) and a summary of the runoff process are also provided (see Tab.1).

Unlike other similar models e.g.: KINEROS (Woolhiser *et al.*, 1990), EUROSEM (Morgan et al., 1998), WEPP (Flanagan and Nearing, 1995; Laflen *et al.*, 1991), HIRM-KW offers flexibility and usability because of the simplicity of its Graphical User Interface (see Fig.6 for a temporary screenshot), designed under MS.NET environment.

Fig.6 – Screenshot of the HIRM-KW Graphic User Interface.

Technically, the numerical core of HIRM-KW is written in standard C++ language (Press et al., 2002), and the GUI (Graphical User Interface) is written in C# (Nash, 2010). The numerical libraries are compiled as .net DLL (Dynamic Link Library) for allowing code portability into other components and applications (Lippman et al., 2000; Malik, 2011).

3.5 The EUROSEM Model

EUROSEM (European Soil Erosion Model) is a single-event, process-based model for predicting soil erosion by water from fields and small cathments (Morgan et al., 1998). The model is based on a physical description of the erosion processes and operates for short time steps of about one-minute. During the simulation, rainfall is first intercepted by the plant canopy and then split into direct throughfall and leaf drainage and stemflow. After determining the kinetic energy of these components, EUROSEM calculates soil splash detachment and models infiltration in accordance with the numerical approach of *Smith* and *Parlange* (1978). Runoff is then routed over the soil surface using the Kinematic-Wave equation accompanied by the modeling of soil erosion as a continuous exchange of particles between the flow and the soil surface. The main model outputs are total runoff, total soil loss, the storm hydrograph and storm sediment graph. An accurate description of the model is provided by Morgan et al. (1998). EUROSEM model was extensively tested by several authors (e.g. Morgan et al., 1998; Folly et

al., 1999; Rosenmund et al., 2005; Mati et al., 2006;Velardo, 2009); the software is freeware and free use and operates with a very rough command line and text interface (DOS like console in all Windows OS).

4. HIRM-KW PERFORMANCES EVALUATION

The current section is dedicated to present the results of some tests made to assess the computing performances of our model. The model validation is beyond the scope of this work.

4.1 Running conditions

Three different simulations were carried out, assuming an overland flow surface subject to the limitations described in Section 3.2.

Tab.2 - Fixed parameters list.

id	Parameters	Symbols	Values	Unit
1	Length of field	L	*160*	m
2	Width of field	W	*120*	m
3	Bed slope	S_0	*0.01*	m/m
4	Soil porosity	Φ	*0.48*	m^3/m^3
5	Basic Manning roughness coef.	n_o	*0.030*	$s/m^{1/3}$
6	Effective net capillary drive	G_0	*526*	mm
7	Initial value of soil water content	θ_I	*0.35*	m^3/m^3
8	surface soil roughness ratio	RFR	*15*	%
9	Saturated soil water content	θ_S	*0.42*	m^3/m^3
10	Net rainfall	R_{NET}	*15*	mm/h
11	Total time of rainfall periods	T_{MAX}	*390*	min

Parameters kept fixed for all simulations are listed in Tab.2, while three values of K_s were taken into account: 2.5, 4.5 and 6.5 mm/h. Moreover, a thin layer of uniform flow was assumed as initial condition.

4.2 Rainfall periods

The overland flow plane was assumed to be subject to a constant rainfall regime of precipitation P_j (mm); each period having equal duration D_j (min). In other words, the rainfall excess was assumed to be uniformly distributed throughout the plane. The test hyetograph is composed by *13* rainfall periods, width a rainfall rate of *15 mm/h*. Then, the total duration is equal to *6.5 h* and the cumulative rainfall, at the end of the simulation, is *97.25 mm*.

4.3 Numerical solution

In the three simulations, a single overland plane was considered as shown in Fig.2 and the Kinematic-Wave model described in Section 3 was used, applying the non-linear implicit numerical scheme given by Eq.(40) and Eq.(33) (or (34)) for the initial estimate of h. The numerical solution of the system was obtained using an *1-minute* time-step ($\Delta t = 1$) and a space-step ($\Delta x \simeq L/N$) about equal to *11.43 m* ($L = 160\,m, N = 14$). This latter value was iteratively calculated by varying the dimensionless parameter N in order to satisfy the numerical stability, finally obtaining *15* equidistant nodes on the entire length (L) of the plane.

4.4 Simulations results comparison

Results of the three simulations described above, were compared with analogous output data produced by EUROSEM model.

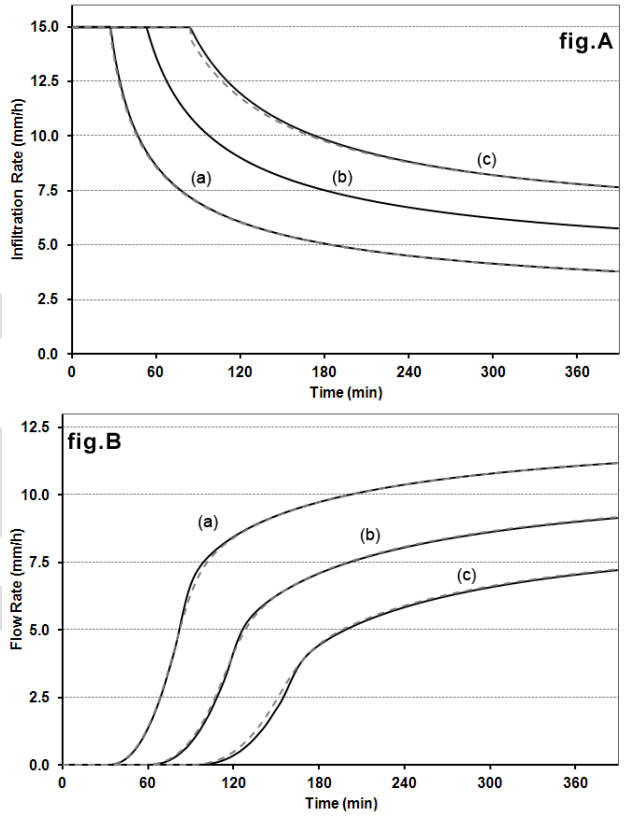

Fig.7 - Comparison between Infiltration capacity $f_c(t)$ (**fig.A**) and Flow Rate $Q(x,t)$ (**fig.B**), simulated by EUROSEM (continuous-line) and HIRM-KW (dashed-line) corresponding to (a) $K_s = 2.5\ mm/h$; (b) $K_s = 4.5\ mm/h$; (c) $K_s = 6.5\ mm/h$.

The comparison is reported in Tab.3, focusing on two key variables: the infiltration capacity $f_c(t)$ and the water flow runoff $Q(x,t)$ (Fig.7).

Tab.3 – EUROSEM and HIRM-KW simulations results.

Rainfall rate 15 mm/h; Slope 1%		*K_S (mm/h)*					
		2.5		*4.5*		*6.5*	
		EUROSEM	*HIRM-KW*	*EUROSEM*	*HIRM-KW*	*EUROSEM*	*HIRM-KW*
Global Volume Balance (mm)	RAIN	*97.25*	*97.25*	*97.25*	*97.25*	*97.25*	*97.25*
	PSTO	*4.97*	*5.04*	*4.42*	*4.44*	*3.85*	*3.82*
	TINF	*40.09*	*40.23*	*56.12*	*56.17*	*69.24*	*69.02*
	TRUN	*52.24*	*52.03*	*36.74*	*36.68*	*24.19*	*24.44*
	TBAL	*97.30*	*97.30*	*97.29*	*97.29*	*97.28*	*97.28*
	GVE %	*-0.049*	*-0.049*	*-0.040*	*-0.040*	*-0.031*	*-0.031*
Hydrology Summary	PRR (mm/h)	*15*	*15*	*15*	*15*	*15*	*15*
	TRUN (min)	*32*	*33*	*59*	*61*	*93*	*93*
	DRUN (min)	*357*	*356*	*330*	*328*	*296*	*296*
	TPFR (min)	*389*	*389*	*389*	*389*	*389*	*389*
	PFR (mm/h)	*11.18*	*11.18*	*9.17*	*9.17*	*7.23*	*7.25*

As clearly displayed, the output of the two models almost coincide for both variables.

5. CONCLUSIONS

This paper can be considered as a useful resource for anyone interested in the mathematical details behind soil water runoff process, as it outlines all steps from the basic laws of motion to the numerical solutions of partial differential equations, describing soil water dynamics.
For what concers its simulation performances, the numerical output provided by HIRM-KW for runoff and infiltration processes was compared with the one produced by EUROSEM (one of the most popular soil erosion models), obtaining a good degree of agreement. Moreover, the HIRM-KW software was developed to be intuitive and simple to use, making it a valuable tool to produce reliable estimates or to support courses on numerical modelling of soil water dynamics, hydrological modelling and water agricultural management.
Finally, it can be easily expanded by removing some of the limitations introduced in Section 3.2 (e.g. by keeping into account cover crops, variable rainfall distributions, wave diffusion for low bottom slopes, etc..), and by adapting it to the agricultural management of water resources.

6. ACKNOWLEDGMENTS

The authors wish to thank *Prof. A. Orefice* (Department of Agricultural and Environmental Sciences - University of Milan, Italy) for his useful comments and remarks.

7. REFERENCES

1. Acutis M., Donatelli M., 2003. SOILPAR 2.0: a software to estimate soil hydrological parameters and functions. European Journal of Agronomy, 18: 373-377.
2. Alaoui A., Germann P., Jarvis N., Acutis M., 2003. Dual-porosity and kinematic wave approaches to assess the degree of preferential flow in an unsaturated soil. Hydrological science 48(3): 455-472.
3. Auerswald K., 1992. Changes in soil surface roughness during erosive rains. Internal report, Lehrstuhl für Bodenkd., TU ünchen, D-8050 Freisning, Germany.
4. Brass R.L., 1990. Hydrology: An Introduction to Hydrologic Science. Addison-Wesley, 643 pp.
5. Bridgman P.W., 1923. Dimensional Analysis. Yale University Press.
6. Brooks R.H., Corey A.T., 1964. Hydraulic properties of porous media. Hydrology Paper n. 3, Colorado State University, Fort Collins (USA), 27 pp.
7. Chow V.T., Maidment D.R., Mays L.W., 1988. Applied Hydrology. Mc Graw-Hill Inc., New York, 572 pp.
8. Chow V.T., 1959. Open-channel hydraulics. McGraw- Hill Book Co., New York, 680 pp.
9. Courant R., Friedrichs K., Lewy H., 1967. On the partial difference equations of mathematical physics. IBM Journal of Research and Development, 11(2): 215–234.
10. Eagleson P.S., 1970. Dynamic Hydrology. McGraw-Hill, Inc., 462 pp.
11. EC (European Commission) 232, 2006. Proposal for a Directive of the European Parliament and of the Council establishing a framework for the protection of soil and amending Directive 2004/35/EC, Brussels, 22 September 2006, COM(2006) 232 final.
12. Epperson J.F., 2002. An introduction to Numerical Methods and Analysis. John Wiley & Sons Inc., 614 pp.
13. Flanagan D.C., Nearing, M.A., 1995. USDA-water erosion prediction project: hillslope profile and watershed model documentation. NSERL Report 10, USDA-ARS National Soil Erosion Research Laboratory, West Lafayette, Indiana, 298 pp.
14. Folly A., Quinton J.N, Smith R.E., 1999. Evaluation of the EUROSEM model using data from the Catsop watershed, The Netherlands. Catena, 37: 507–519.
15. Govindaraju R.S., Jones S.E., Kavvas M.L., 1988a. On the diffusion wave model for overland flow 1. Solution for steep slopes. Water Resour. Res., 24(5): 734-744.
16. Govindaraju R.S., Jones S.E., Kavvas M.L., 1988b. On the diffusion wave model for overland flow 2. Steady state analysis. Water Resour. Res., 24(5): 745–754.
17. Henderson F.M., 1966. Open channels Flow. Mcmillan, New York.
18. Hillel D., 1980. Fundamentals of soil physics. Acc. Press Inc., London, 413 pp.
19. Holden A.P, Sthephenson D., 1988. Improved four-point solution of kinematic equations. Journal of Hydraulic Research, 26(4): 413-423.
20. Holden A.P, Sthephenson D., 1995. Finite difference formulations of kinematic equations. Journal of Hydraulic Research, 121(5): 423-426.
21. Huber W.C., Dickinson R.E., 1988. SWMM Version 4 User's Manual. US Environmental Protection Agency.
22. Kazezyilmaz-Alhana C.M., Medina M.A, Rao P., 2005. On numerical modeling of overland flow. Appl. Math. Comp., 166(3): 724-740.
23. Kibler D.F, Woolhiser D.A., 1970. The Kinematic cascade as a hydrologic model. Hydrology Paper n. 39, Colorado State University, 27 pp.
24. Laflen J.M., Lane L.J., Foster G.R., 1991. WEPP: A new generation of erosion prediction technology. J. Soil Water Conserv., 46: 30-34.
25. Lax P.D., Richtmyer R.D., 1956. Survey of the stability of linear finite difference equations. Comm. Pure Appl. Math., 9: 267-293. MR 79204, DOI 10.1002/cpa.3160090206.
26. Liggett J.A., Cunge J.A., 1975. Numerical methods of solution of the unsteady flow equations. In Yevjevich (Eds), Unsteady flow in open channels, vol. I. Water Resources Publisher, Ft Collins Colorado: 89-179.
27. Linsley R.K., Kohler M.A., Paulus J.L.H., 1982. Hydrology for Engineers. McGraw-Hill Book Co., New York, 508 pp.
28. Lippman S.B., and Lajoie J., 2000. C++ Corso di Programmazione, 3a Ed., Addison-Wesley Longman Italia, 1209p., ISBN: 88-7192-071-6.
29. Malik D.S., 2011. C++ Programming: Program Design Including Data Structures, Fifth Edition. Course Technology, 1573p., ISBN-13: 978-0-538-79809-2.
30. Mati B.M., Morgan R.P.C., and Quinton J.N., 2006. Soil erosion modelling with EUROSEM at Embori and Mukogodo catchments, Kenya. Earth Surf. Process. Landforms, 31,

579-588. DOI:10.1002/esp.1347.
31. Miller J.E., 1984. Basic Concepts of Kinematic-Wave Models. US Geo. Survey Prof. Paper 1302, 36 pp.
32. Moramarco T., Singh V.P., 2002. Accuracy of kinematic wave and diffusion wave for spatial-varying rainfall excess over a plane. Hydrol. Process., 16: 3419-3435. DOI 10.1002/hyp.1108.
33. Morel-Seytoux H.J., Meyer P.D., Nachabe M., Touma J., van Genuchten M.T., and Lenhard R.J. 1996. Parameter equivalence for the Brooks-Corey and van Genuchten soil characteristics: Preserving the effective capillary drive. Water Resources Research, 32 (5): 1251-1258.
34. Morel-Seytoux H.J., Nimmo J.R., 1999.Soil water retention and maximum capillary drive from saturation to oven dryness. Water Resources Research, 35 (7): 2031-2041.
35. Morgan R.P.C., Quinton J.N., Smith R.E., Govers G., Poesen J.W.A., Auerswald K., Chisci G., Torri D., Styczen M.E., Folly A.J.V., 1998. The European Soil Erosion Model (EUROSEM): A Dynamic Approach for Predicting Sediment Transport from Fields and Small Catchments. Earth Surf. Process. Landforms, 23: 527–544.
36. Mualem Y., 1976. A new model for predicting the hydraulic conductivity of unsaturated porous media. Water Resources Research, 12: 513-522.
37. Nash T., 2010. Accelerate C# 2010. Spring-Verlag, NY, 627 pp. ISBN 978-1-4302-2538-6.
38. Ogden F.L., Julien P.Y., 1993. Runoff Sensitivity to Temporal and Spatial Rainfall Variability at Runoff Plane and Small Basin Scales. Water Resources Research, 29(8): 2589-2597.
39. Ogden F.L., Saghafian B., 1997. Green and Ampt Infiltration with Redistribution. J. Irr. Drain. Eng., 123: 386-393.
40. Parlange J.Y., 1971. Theory of water movement in soils: 2. One dimensional infiltration. Soil Sci., 111: 170-174.
41. Parlange J.Y., 1972. Theory of water movement in soils: 8. One-dimensional infiltration with constant flux at the surface. Soil Sci., 114: 1-4.
42. Parlange J.Y., 1975a. Theory of water movement in soils: 11. Conclusion and discussion of some recent developments. Soil Sci., 119: 158-161.
43. Parlange J.Y., 1975b. On solving the flow equation in unsaturated soils by optimization: Horizontal infiltration. Soil Sci. Soc. Am. Proc., 39: 415-418.
44. Parlange J.Y., Lisle I., Braddock R.D., Smith R.E., 1982. The three-parameter infiltration equation. Soil Sci., 133: 337–341.
45. Perego A., Giussani A., Sanna M., Fumagalli M., Carozzi M., Alfieri L., Brenna S., Acutis M., 2013. The ARMOSA simulation crop model: overall features, calibration and validation results. Italian Journal of Agrometeorology, 3: 23-38.
46. Ponce V.N., Indlekofer H., Simons D.B., 1978. Convergence of four-point implicit water wave model. Journal of the Hydraulics Division, ASCE, 104, (HY7): 947-958.
47. Preissmann A., 1961. Propagation of translator waves in channels and rivers. Proceedings, First Congress of the French Association for Computation, Grenoble, France: 433-442.
48. Press W.H., Teukolsky S.A., Vetteling W.T, Flannery B.P., 2002. Numerical Recipes in C++: The Art of Scientific Computing, 2nd Ed. Cambridge University Press, 1002 pp. ISBN 0-521-75033-4.
49. Rawls W.J., Pachepsky Y., 2004. Development of Pedotransfer Functions in Soil Hydrology (Developments in Soil Science). Elsevier Science Ltd, 542 pp.
50. Rawls W.J., Brakensiek D.L., Saxton K.E., 1982. Estimation of soil water properties. Trans. ASAE, 25: 1316–1330.
51. Richtmyer R.D., Morton K.W., 1967. Difference Methods for Initial-Value Problems. 2nd ed. Wiley (Interscience), New York.
52. Rosenmund A., Confalonieri R., Roggero P.P., Toderi M., Acutis M., 2005. Evaluation of the EUROSEM model for simulating erosion in hilly areas of Central Italy. Italian Journal of Agrometeorology, 2: 15-23.
53. Saxton K.E., Rawls W.J., Romberger J.S., Papendick R.I., 1986. Estimating generalized soil-water characteristics from texture. Soil Sci. Am. J., 50: 1031-1036.
54. Singh V.P., 1996. Kinematic Wave Modeling in Water Resource. Surface-Water Hydrology. John Wiley e Sons. Inc, 1399 pp. ISBN 0-471-10945-2.
55. Singh VP., 2002. Is hydrology kinematic? Hydrol. Process. 16, 667–716. DOI: 10.1002/hyp.306.
56. Smith R.E., 2002. Infiltration Theory for Hydrologic Applications. Water Resources Monograph 15, AGU.
57. Smith R.E., Parlange Y.Y., 1978. A parameter-efficient hydrologic infiltration model. Water Resources Research, 14 (3): 533-538.
58. Smith G.D., 1985. Numerical Solution of Partial Differential Equations: Finite Difference Methods / Edition 3. Publisher Oxford University Press, USA. ISBN 13-9780198596509.
59. Stephenson D., Meadows M.E., 1986. Kinematic Hydrology and Modeling. Elsevier, Amsterdam, 250 pp.
60. Strikwerda J.C., 2004. Finite Difference Schemes and Partial Differential Equations. 2nd Edition. SIAM, 435 pp. ISBN 0-89871-567-9.
61. Thomas W., 1995. Numerical Partial Differential equation: finite difference methods. Springer-Verlag, New York.
62. Van Genuchten M.T., 1980. A closed-form equation for predicting the hydraulic conductivity of unsaturated soils. Soil Sci. Soc. Am. J., 44: 892-898.
63. Velardo M.C., 2009. Water surface runoff from agricultural systems: measurement and modellization of amounts, solid transport and nutrient content. Ph.D-thesis in Agricultural Ecology XXII Cycle. University of Milan, Italy.
64. Wood W.L., 1993. Introduction to Numerical Methods for Water Resources. Oxford University Press 255 pp. ISBN 0-19-859690-1.
65. Woolhiser D.A., Liggett J.A., 1967. Unsteady one-dimensional fow over a plane: the rising hydrograph. Water Resources Research 3(3): 753-771.
66. Woolhiser D.A., Anson C.L., Kuhlman A.R., 1970. Overland Flow on Rangeland Watersheds. Journal of Hydrology, 9 (2): 336-356.
67. Woolhiser D.A., Smith R.E., Goodrich D.C., 1990. KINEROS, a Kinematic Runoff and Erosion Model: Documentation and User Manual. United States Department of Agriculture, ARS-77.
68. Yen B.C., Chow V.T., 1974. Experimental Investigation of Watershed Surface Runoff. Hydraulic Engineering Series, N.29, Dept. of Civil Engineering, University of Illinois at Urbana- Champaign.

APPENDIX A: BASIC FLOW-ROUTING EQUATIONS

A.1 – Dynamic Wave models

The equations of motion for free surface (or open-channel) flows in *non-stationary* conditions are commonly referred to as *Dynamic-Wave* equations. Dynamic-Wave models of surface runoff assume that the motion is described by a succession of instantly locally non-uniform motions, slowly varying in space and time (Eagleson, 1970; Chow *et al.*, 1988; Brass, 1990; Linsley *et al.*, 1982).

In the one-dimensional form, they include the *dynamic momentum equation*:

$$\frac{\partial U}{\partial t} + g\frac{\partial h}{\partial x} + U\frac{\partial U}{\partial x} - g(S_0 - S_f) = 0 \qquad \text{(A.1.1)}$$

where external inputs are negligible (Eagleson, 1970), and the *continuity equation*:

$$\frac{\partial A}{\partial t} + \frac{\partial Q}{\partial x} = q_E,\ Q = UA \qquad \text{(A.1.2)}$$

By definition, $Q(x,t)$ $[L^3/T]$ is the volumetric flow rate crossing a section with velocity $U(x,t)$ per time unit t; $U(x,t)$ $[L/T]$ is the average speed of the flow section in the direction of motion; $h(x,t)$ $[L]$ is the portion of free surface (or flow depth) with respect to a reference plane; $A(x,t)$ $[L^2]$ is the area of the liquid cross-section; S_f is the (dimensionless) friction slope (i.e. the rate at which energy is lost along a given length channel); $S_0 = \tan\vartheta$ is bed slope (where $0 \le \vartheta \le 90°$ is the inclination angle in degrees); g $[L/T^2]$ is the gravity acceleration; t is time; x is the horizontal coordinate oriented in the direction of motion; $q_E(x,t)$ $[L^2/T]$ is the sum of the flows entering and leaving the section (also called *lateral flow*).

In order to solve the system (A.1.1)-(A.1.2) and consequently find a solution for $Q(x,t)$, it is necessary to know the average speed variation as a function of the independent variables t and x.

For the open-channel flow several empirical formulas exist, holding for the cross-section averaged flow velocity (Henderson, 1966; Chow, 1959). The most common ones the *Chezy* formula and the *Manning* formula, which can be expressed with the following general formulation:

$$U = N\sqrt{S_f}{R_a}^{\beta-1} \equiv \frac{N\sqrt{S_f}}{P^{\beta-1}}A^{\beta-1} \qquad \text{(A.1.3)}$$

where $R_a = A/P$ $[L]$ is the hydraulic radius, defined as the flow cross-sectional area A divided by the wetted perimeter P $[L]$ of A and β is an *index of nonlinearity*. If the *Chezy* relationship is used, then $\beta \equiv \frac{3}{2}$ and $N \equiv C$ (*Chezy* roughness coefficient C has the dimensions $\left[L^{1/2}/T\right]$). If the *Manning* relationship is used, then $\beta \equiv \frac{5}{3}$, and $\frac{1}{N} \equiv n$ (*Manning* roughness coefficient n as the dimensions $\left[T/L^{1/3}\right]$).

In natural channels n and C depend both on the geometry and the roughness of the wet perimeter; in cultivated land they also depend on surface roughness and vegetation cover.

From the definition $Q = UA$ and from the (*Manning* or *Chezy*) law of resistance (A.1.3) we obtain

$$Q = \alpha\, A^{\beta} \qquad \text{(A.1.4)}$$

where

$$\alpha \equiv \frac{N\sqrt{S_f}}{P^{\beta-1}} \equiv \frac{N}{P^{\beta-1}}\sqrt{S_0 - \frac{1}{g}\left(\frac{\partial U}{\partial t} + g\frac{\partial h}{\partial x} + U\frac{\partial U}{\partial x}\right)} \qquad \text{(A.1.5)}$$

substituting (A.1.4) into (A.1.2)

$$\frac{\partial A}{\partial t} + \frac{\partial}{\partial x}\left(\alpha A^{\beta}\right) = q_E \qquad \text{(A.1.6)}$$

differentiating the second partial derivative of (A.1.6)

$$\frac{\partial}{\partial x}\left(\alpha A^{\beta}\right) = \alpha\frac{\partial}{\partial x}A^{\beta} + A^{\beta}\frac{\partial \alpha}{\partial x} \qquad \text{(A.1.7)}$$

performing the derivative

$$\frac{\partial}{\partial x}A^{\beta} = \beta A^{\beta-1}\frac{\partial A}{\partial x} \qquad \text{(A.1.8)}$$

and substituting (A.1.8) into (A.1.7) finally leads

$$\frac{\partial A}{\partial t} + \beta\alpha A^{\beta-1}\frac{\partial A}{\partial x} + A^{\beta}\frac{\partial \alpha}{\partial x} = q_E \qquad \text{(A.1.9)}$$

Eqs.(A.1.4) and (A.1.9) are called *Dynamics-Wave* equations.

A.2 – Approximate form of the Dynamic-Wave equation

When the convective accelerations of a slow flow in non-uniform motion through a section A are *only* locally negligible and both $\partial U/\partial t$ and $\partial U/\partial x$ in (A.1.1) are approximately zero, the friction slope S_f can be approximated as follows:

$$S_f \approx S_0 - \frac{\partial h}{\partial x} \equiv \hat{S}_f,\ \ (S_0 = \tan\vartheta) \qquad \text{(A.2.1)}$$

For a *wide channel of rectangular section*, having width W and height equal to the flow depth h, the cross section is equal to $A = Wh$, and the wet perimeter becomes $P = 2h + W$. So that, (A.1.9) can be re-written as:

$$\frac{\partial h}{\partial t} + \beta\alpha_C h^{\beta-1}\frac{\partial h}{\partial x} + h^{\beta}\frac{\partial \alpha_C}{\partial x} = \tilde{q}_E \qquad \text{(A.2.2)}$$

where $\tilde{q}_E \equiv q_E/W$ [L/T] is a *flow speed* (i.e. flow per unit width W) and

$$\alpha_C(x,t) \equiv \left(\frac{W}{2h+W}\right)^{\beta-1} N\sqrt{\hat{S}_f} \qquad \text{(A.2.3)}$$

Now combining (A.2.3) with (A.1.4) we get

$$Q = W\alpha_C h^{\beta} \qquad \text{(A.2.4)}$$

In other words, the general discharge rate Q depends on both h and the gradient $\partial h/\partial x$ through the term $\hat{S}_f$. Eq.(A.2.2) is referred to as *Diffusion-Wave* equations.

A.3 – Approximate form of the Diffusion-Wave equation

The Manning and Chezy resistance law (A.2.3) for the Diffusion-Wave (A.2.2) can be written as:

$$\alpha_C(x,t) = R\sqrt{S_f} \cong R\sqrt{S_0 - \frac{\partial h}{\partial x}} \qquad \text{(A.3.1)}$$

where

$$R \equiv \begin{cases} \left(\frac{W}{2h+W}\right)^{\beta-1} C,\ \ \beta \equiv \frac{3}{2}\ \ (Chezy) \\ \left(\frac{W}{2h+W}\right)^{\beta-1}\frac{1}{n},\ \ \beta \equiv \frac{5}{3}\ \ (Manning) \end{cases} \qquad \text{(A.3.2)}$$

If R is constant (or $W >> h$), then the second term of (A.2.2) can be expanded as follows

$$\frac{\partial \alpha_c}{\partial x} = R\frac{\partial}{\partial x}\left(S_f{}^{1/2}\right) = \frac{R}{2S_f{}^{1/2}}\frac{\partial S_f}{\partial x} \quad (A.3.3)$$

then calculating

$$\frac{\partial S_f}{\partial x} = \frac{\partial}{\partial x}\left(S_0 - \frac{\partial h}{\partial x}\right) = -\frac{\partial}{\partial x}\left(\frac{\partial h}{\partial x}\right) = -\frac{\partial^2 h}{\partial x^2} \quad (A.3.4)$$

and substituting into Eq.(A.3.3)

$$\frac{\partial \alpha_c}{\partial x} = -\frac{R}{2S_f{}^{1/2}}\frac{\partial^2 h}{\partial x^2} = -\frac{\alpha_c}{2S}\frac{\partial^2 h}{\partial x^2} \quad (A.3.5)$$

we are finally able to obtain the diffusive term of (A.2.2) in the form

$$h^\beta \frac{\partial \alpha_c}{\partial x} = -h^\beta \frac{\alpha_c}{2S}\frac{\partial^2 h}{\partial x^2} = -k(h)\frac{\partial^2 h}{\partial x^2} \quad (A.3.6)$$

substituting (A.3.6) into Eq.(A.2.2), the Diffusion-Wave can be written as:

$$\frac{\partial h}{\partial t} + c_K(h)\frac{\partial h}{\partial x} - k(h)\frac{\partial^2 h}{\partial x^2} = \tilde{q}_E \quad (A.3.7)$$

where

$$c_K(h) \equiv \beta\alpha_C h^{\beta-1}, \;\; k(h) \equiv \frac{\alpha_C}{2\hat{s}_f}h^\beta \quad (A.3.8)$$

The coefficients c_K $[L/T]$ and k $[L^2/T]$ are the *celerity* and the *hydraulic diffusivity* of the *approximate form* of the Diffusion-Wave (DW), respectively.
In (A.3.7), the flow is *convective-diffusive*, while the extra term $k(h)\frac{\partial^2 h}{\partial x^2}$ is a standard form of Diffusion-Wave equation, arising from the inclusion of the pressure term in (A.2.1).
(A.3.7) is formally similar to equations (11.34), (11.39) and (11.41) proposed by Singh (1996).

A.4 – Kinematic Wave approximation

The most radical approximation in Eqs.(A.2.2) and (A.3.7), known as the *Kinematic-Wave* (KW) approximation, neglects any inertial and gravitational effect induced by non-parallelism between the free surface and the bottom of the flow. At regime, the motion is considered as *uniform*, so the flow conditions at each point do not depend on time.
As a consequence, friction slope and bed slope are approximately equal, and (A.1.1) and (A.2.1) can be approximated by:

$$S_f \approx S_0 \equiv \tan\vartheta \quad (A.4.1)$$

A.4.1.- Channels with arbitrary section

When the approximation (A.4.1) is applied to a free surface channel, (A.1.4) is drastically simplified to:

$$Q = \frac{N\sqrt{S_0}}{P^{\beta-1}}A^\beta \equiv \alpha_C A^\beta \quad (A.4.2)$$

Recalling (A.1.5), if the *Chezy* relationship is used, then $\alpha_C \equiv C\sqrt{S_0}/P^{\beta-1}$; on the other hand, if the *Manning* relationship is used, then $\alpha_C \equiv \sqrt{S_0}/nP^{\beta-1}$.
Dealing with motion in channels of arbitrary section, it is more appropriate to write the Kinematic-Wave equation in terms of Q. We get then, from Eq.(A.4.2):

$$A = \alpha_* Q^{\beta_*} \quad (A.4.3)$$

where $\alpha_* \equiv (1/\alpha_C)^{\beta_*}$, and $\beta_* \equiv 1/\beta$. According to (A.3.2), $\beta_* \equiv 3/5$ in the *Manning* formula and $\beta_* \equiv 2/3$ in the *Chezy* formula. Combining (A.4.2) with the continuity equation (A.1.2), we can conclude:

$$\frac{\partial Q}{\partial t} + c_K\frac{\partial Q}{\partial x} = c_K q_E \quad (A.4.4)$$

where

$$c_K \equiv \frac{1}{\alpha_*\beta_* Q^{\beta_*-1}} \quad (A.4.5)$$

Eq.(A.4.4) is the most common form of the Kinematic-Wave equation, used to calculate an open-channel flow passing through any channel section, under the assumption of uniform motion.

A.4.2.- Channels with a rectangular section

Because of the approximation (A.4.1), the coefficient α_C in (A.2.2) includes only the assigned parameters n (or C), P and S_0. It follows that $\partial\alpha_C/\partial x = 0$, and consequently:

$$\frac{\partial h}{\partial t} + c_K\frac{\partial h}{\partial x} = \tilde{q}_E \quad (A.4.6)$$

where

$$c_K \equiv \beta\alpha_C h^{\beta-1} \quad (A.4.7)$$

In this case the discharge rate Q is defined by (A.4.2), namely the Kinematic-Wave approximation for uniform flows across rectangular section channels.

A.4.3.- Wave Celerity of the Kinematic-Wave equation

From a physical point of view, *celerity* is the speed at which the wave propagates in the direction of motion; in other terms, it is the celerity at which a wave crosses a section A. Celerity c_K has the dimensions of $[L/T]$ and derives from the definition of wave velocity $c_K = dx/dt$ leading to $c_K = \beta U(x,t)$ where U $[L/T]$ is the average wave propagation speed (Singh, 1996).
In the Kinematic-Wave models (A.4.4) and (A.4.6) , celerity c_K defined by

$$c_K = \beta U(x,t) \quad \begin{cases} \equiv \beta\alpha_C h^{\beta-1} \;\; (planes) \\ \equiv \beta\frac{\alpha_C^{1/\beta}}{Q^{(1-\beta)/\beta}}, \;\; (channels) \end{cases} \quad (A.4.8)$$

Clearly, celerity c_K is a function of the flow depth h and of the resistance law adopted (see e.g. Singh, 1996; Brass, 1990; Chow, 1982). In the explicit numerical finite difference schemes, the wave celerity is used to control numerical stability.

A.4.4.- Criterion of applicability of the Kinematic-Wave model

Woolhiser and Liggett (1967) have derived a criterion for judging the goodness of kinematic wave approximation in modelling flow over a sloping plane subject to rainfall or lateral inflow.
The criterion of applicability of the Kinematic-Wave model is based on two *dimensionless* coefficients:

the *Froude number*, defined by

$$F_r{}^2 = \frac{U^2}{gh_L} \quad (A.4.9)$$

and the *Kinematic flow number*, defined by

$$K = \frac{L\,S_0}{h_L\,F_r{}^2} \equiv \frac{L\,S_0\,g}{U^2} \quad (A.4.10)$$

where S_0 is the bed slope of plane; L is the length of plane or

channel, g is the gravity acceleration, h_L is the flow height at $x = L$. Sometimes these two parameters are indicated by $F_r{}^2 K \equiv L\, S_0 / h_L$.

In planes or channels with rectangular section, (A.4.9)-(A.4.10) can be based on physically significant and measurable parameters:

$$K \equiv \frac{g\, n^{1.2} {S_0}^{0.4} L^{0.2}}{{i_{max}}^{0.8}};\quad F_r \equiv \frac{{S_0}^{0.45} (L\, i_{max})^{0.1}}{n^{0.9}\sqrt{g}}. \qquad (A.4.11)$$

if the *Manning* formula is used.

$$K \equiv \frac{g\,(S_0\, L)^{0.33}}{C^{1.33}\, {i_{max}}^{0.66}};\quad F_r \equiv C\,\sqrt{\frac{S_0}{g}} \qquad (A.4.12)$$

if the *Chezy formula* is used. The term i_{max} $[L/T]$ is the maximum rate of lateral inflow.

As we already known, it is defined as the maximum specific intensity $i_{max} = P_{max}/D_{max}$, where P_{max} is the maximum precipitation amount, occurring in the D_{max} time interval.

A.4.5.- Estimation of Manning coefficient n

Manning coefficient n is used in HIRM-KW to describe the roughness imparted to the flow and its value represents the summation of roughness (friction) effects (Chow, 1959):

$$n \cong (n_0 + n_g + n_v + n_m) m_n \qquad (A.4.13)$$

where n_0 is the initial roughness coefficient, n_g is the grain roughness due to the soil particles, n_v is the roughness imparted by vegetation, and n_m is the micro-topographic roughness of the soil surface; m_n is a parameter ranging between 1.0 (bare soil) and 1.2. Since n cannot be directly measured, its value needs to be estimated.

In general, standard textbooks (e.g., Chow, 1959; Linsley *et al.*, 1982) provide typical n values for open-channel flow.

A.5 – Derivation of effective capillary drive G, from Eq.(13)

By substituting Brooks and Corey Eqs.(13) into Eq.(12) and integrating between θ_I and θ, we get

$$G(\theta) = \int_{\theta_I}^{\theta} \vartheta(\theta)^{3+2/\lambda} \left(\frac{d\psi}{d\theta}\right) d\theta \qquad (A.5.1)$$

where

$$\vartheta(\theta) = \frac{\theta - \theta_r}{\theta_s - \theta_r} = \left(\frac{\Psi_B}{\psi}\right)^{\lambda} \qquad (A.5.2)$$

(dimensionless) is the relative volumetric water content of the soil profile with suction head ψ. The derivative $\frac{d\psi}{d\theta}$ can be evaluated by

$$\frac{d\psi}{d\theta} = -\frac{\psi_B}{\lambda\, \vartheta^{1+1/\lambda}} \frac{d\vartheta}{d\theta} \qquad (A.5.3)$$

Then, by substituting (A.5.3) into (A.5.1) we get

$$G(\theta_I, \theta) = -\frac{\psi_B}{\lambda} \int_{\theta_I}^{\theta} \frac{\vartheta^{3+2/\lambda}}{\vartheta^{1+1/\lambda}} d\vartheta \equiv -\frac{\psi_B}{\lambda} \int_{\theta_I}^{\theta} \vartheta^{2+1/\lambda} d\vartheta \qquad (A.5.4)$$

In the end, Eq.(A.5.4) can be obtained by performing the definite integral (Ogden et al., 1997):

$$G(\theta_I, \theta) = -\frac{\psi_B}{\lambda} \left(\frac{\vartheta^{3+1/\lambda} - {\vartheta_I}^{3+1/\lambda}}{3+1/\lambda} \right) \qquad (A.5.5)$$

Note that when $\psi \to 0$ (at the saturation) then $\theta \to \theta_S$ end $\vartheta(\theta) \equiv 1$ and consequently Eq.(A.5.5) reduced to Eq.(14).

APPENDIX B: FINITE DIFFERENCE METHODS (FDM)

Finite differencing is a technique thanks to which continuous phenomena can be approximated by discrete functions. The basic FDM idea is to replace each derivative with a finite incremental ratio (see e.g. Strikwerda, 2004; Holden and Stephenson, 1995; Smith, 1995).

Doing so a PDE can be converted into an algebraic equation involving values assumed by the equation variables at certain discrete points in space and time (Figs.B).

Such discrete points are often called *nodes* and the intervals in space and time are called *mesh increments*. Nodes and mesh increments form a *solution mesh*. The mesh increment size may or may not be equal in all spatial directions used, and they may or may not be uniform throughout the solution mesh (Hillel, 1980, Smith, 1985).

The main additional restriction of a finite difference model is its *accuracy*, in comparison with the solution of PDE itself. However, if a finite-difference model is valid, then it converges to the PDE as the mesh increments approach to zero (Richtmyer and Morton, 1967).

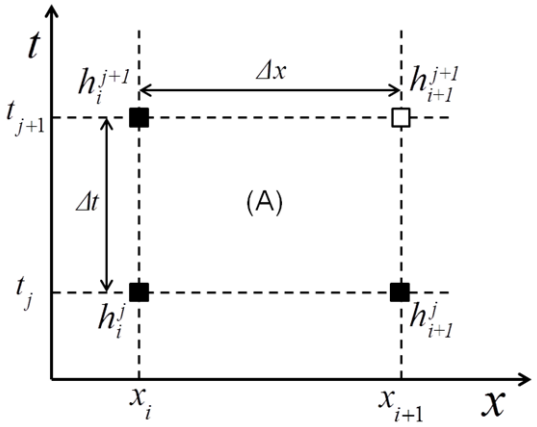

Fig.B.1: solution mesh of the linear 3-points FDB scheme. The unknown node h_{i+1}^{j+1} is determinate by known node h_i^j, h_i^{j+1}, h_{i+1}^j.

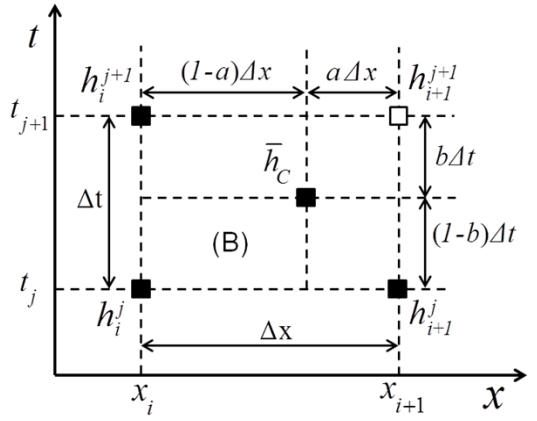

Fig.B.2: solution mesh of the nonlinear 4-points FD scheme. In this case the unknown node h_{i+1}^{j+1} can be determinate only by using an iterative method.

Different approximations for the derivatives lead to different numerical schemes: *Full Implicit/Explicit, Lax-Friedrichs, Crank-Nicolson, Preissmann*, etc.

Depending on the solving scheme of the problem, these methods are divided in two types: *implicit* and *explicit*. In the first case, the

solution is directly found by linearly expressing the variable to be determined; in the second case, the solution is obtained iteratively by non-linear methods (e.g. Press *et al.*, 2002; Epperson, 2002; Liggett and Cunge, 1975).

Fig.B.1 shows the FDB of the *linear 3-points scheme*, while Fig.B.2 displays the *nonlinear 4-points FD scheme*, where "a" and "b" are the *weight factors* of the partial derivatives (see e.g. Singh, 1996; Preissmann, 1961; Wood, 1993; Holden and Stephenson, 1988, 1995).

The explicit finite differences schemes lend themselves to approximate problems of linear type, or related to linear type. They have the disadvantage of easily becoming unstable, meaning the inevitable approximation errors become so large that the solution is destroyed (Linsley *et al.*, 1982). Since it is often difficult, or even impossible, to prove the convergence of a numerical method (i.e. the existence of a unique approximated solution), hence a less restrictive (necessary but not sufficient) stability condition is generally imposed. This restriction is called *Courant- Friedrichs-Lewy Condition* (Courant *et al.*, 1967), and the corresponding explicit schemes are called *conditionally stable*. In an explicit scheme the pattern on the discretized plane (x_i, t_j) is built with time step Δt, and spatial step Δx, which have to be adequately chosen at the beginning of calculation. The subscripts *i* and *j* denote incremented space and time levels, respectively.

B.1 – Linear 3-points FDB schemes of Eq.(33)

If the initial conditions are the nodal points h_i^j, h_i^{j+1}, h_{i+1}^j then we obtain an *implicit linear three-point backward scheme* and the *FD* approximations for the derivative is given by:

$$\begin{aligned}
&\frac{\partial h}{\partial t} \approx \frac{h_{i+1}^{j+1} - h_{i+1}^{j}}{\Delta t} \qquad (backward\ in\ time),\\
&\frac{\partial h}{\partial x} \approx \frac{h_{i+1}^{j+1} - h_{i}^{j+1}}{\Delta x} \qquad (backward\ in\ space),\\
&\bar{q}_E \approx 0.5\left(q_{i+1}^{j} + q_{i}^{j+1}\right),\\
&q_{i+1}^{j} \equiv (i-f)_{i+1}^{j},\ \ q_i^{j+1} \equiv (i-f)_i^{j+1}.
\end{aligned} \tag{B.1.1}$$

B.2 – Linear 3-points FDB schemes of Eq.(34)

If the initial conditions correspond to the nodal points h_i^j, h_i^{j+1}, h_{i+1}^j, we obtain an *explicit linear three-point backward* scheme of the form:

$$\begin{aligned}
&\frac{\partial h}{\partial t} \approx \frac{h_{i+1}^{j+1} - h_{i+1}^{j}}{\Delta t} \qquad (backward\ in\ time),\\
&\frac{\partial h}{\partial x} \approx \frac{h_{i+1}^{j} - h_{i}^{j}}{\Delta x} \qquad (bakward\ in\ space),\\
&\bar{q}_E \approx 0.5\left(q_{i}^{j+1} + q_{i}^{j}\right),\\
&q_{i}^{j} \equiv (i-f)_{i}^{j},\ \ q_i^{j+1} \equiv (i-f)_i^{j+1}.
\end{aligned} \tag{B.2.1}$$

B.3 – Nonlinear 4-points FD Schemes of Eq.(37)

In order to reduce the problems of numerical stability and convergence in linear explicit systems, various authors suggest the employment of nonlinear implicit schemes, which turn out to be much more stable. These schemes are classified as *unconditionally stable* and they are not subject to the *Courant-Friedrichs-Lewy* condition (Ponce *et al.*, 1978). Considering h as a variable of the system and referring to the scheme of Fig.B.2, the terms h, q_E, $\frac{\partial h}{\partial x}$ and $\frac{\partial h}{\partial t}$, can be approximated as follows (Preissmann, 1961; Holden and Stephenson, 1988, 1995; Wood, 1993):

$$\begin{aligned}
&\frac{\partial h}{\partial t} \approx \frac{(1-a)}{\Delta t}\left(h_{i+1}^{j+1} - h_i^j\right) + \frac{a}{\Delta t}\left(h_{i+1}^{j+1} - h_{i+1}^{j}\right),\\
&\frac{\partial h}{\partial x} \approx \frac{(1-b)}{\Delta x}\left(h_{i+1}^{j} - h_i^j\right) + \frac{b}{\Delta x}\left(h_{i+1}^{j+1} - h_i^{j+1}\right)
\end{aligned} \tag{B.3.1}$$

and (B.3.2)

$$\begin{aligned}
&h \approx (1-b)\left(a h_{i+1}^{j} + (1-a) h_i^j\right) + b\left(a h_{i+1}^{j+1} + (1-a) h_i^{j+1}\right)\\
&q_E \approx (1-b)\left(a q_{i+1}^{j} + (1-a) q_i^j\right) + b\left(a q_{i+1}^{j+1} + (1-a) q_i^{j+1}\right)
\end{aligned}$$

where h_i^j, h_i^{j+1}, h_{i+1}^j are the assigned nodal points; h_{i+1}^{j+1} is indirectly calculated from known points; a is the space weighting parameter; b is the time weighting parameter (see Fig.B.2). The coefficients a and b are dimensionless, ranging between 0 and 1 (typical values are $0.6 \le b \le 0.7$ and $a = 0.5$ - Ponce *et al.*, 1978).

By assigning suitable values to a and b in (B.3.1), different implicit and explicit patterns can be obtained (e.g., setting $a = 1/2$ and $b = 1$ results in a fully explicit numerical scheme).

Modified Preissmann scheme

A widely employed variant of formulas (B.3.1) and (B.3.2) derives by setting $a \equiv \frac{1}{2}, 0.6 \le b \le 1$, resulting in the 4-points implicit scheme:

$$\begin{aligned}
&\frac{\partial h}{\partial t} \approx \frac{\left(h_{i+1}^{j+1} - h_{i+1}^{j} + h_i^{j+1} - h_i^{j}\right)}{2\Delta t},\\
&\frac{\partial h}{\partial x} \approx \frac{(1-b)}{\Delta x}\left(h_{i+1}^{j} - h_i^j\right) + \frac{b}{\Delta x}\left(h_{i+1}^{j+1} - h_i^{j+1}\right)
\end{aligned} \tag{B.3.3}$$

and

$$\begin{aligned}
&h \approx \tfrac{1}{2}\left[b\left(h_{i+1}^{j+1} - h_i^{j+1}\right) + (1-b)\left(h_{i+1}^{j} - h_i^{j}\right)\right],\\
&q_E \approx b\bar{q}^{\,j+1} + (1-b)\bar{q}^{\,j}\\
&\bar{q}^{\,j+1} \equiv \tfrac{1}{2}\left(q_{i+1}^{j+1} + q_i^{j+1}\right),\ \ \bar{q}^{\,j} \equiv \tfrac{1}{2}\left(q_{i+1}^{j} + q_i^{j}\right),
\end{aligned} \tag{B.3.4}$$

where the terms $\frac{\partial h}{\partial x}$, h and q_E are *weighted* by b.